Application of industrial waste based catalysts for total oxidation of propane

S. Sushil [a], P. Scholz [b], K. Pollok [c], B. Ondruschka [b], V.S. Batra [a],*

[a] Center for Energy and Environment, TERI University, Darbari Seth Block, Habitat Place, Lodhi Road, New Delhi 110003, India
[b] Friedrich-Schiller-Universität Jena, Institut für Technische Chemie und Umweltchemie, Lessingstraße 12, D-07743 Jena, Germany
[c] Bayerisches Geoinstitut, Universität Bayreuth, D-95440 Bayreuth, Germany

ARTICLE INFO

ABSTRACT

High metal containing wastes from the aluminium industry, the tannery industry and the electroplating industry were tested as precursors for catalysts. These waste materials were processed using various treatments and tested for the total oxidation of volatile organic compounds employing propane as a model gas. Comparisons were made with unprocessed counterparts in certain cases. Investigations were made in the temperature range of 100–500 °C with a GHSV of 5000 h^{-1}. Characterization of fresh and used catalysts was performed using techniques like BET analysis, X-ray diffraction (XRD), X-ray fluorescence (XRF), inductively coupled plasma optical emission spectrometry (ICP-OES) and thermal analyses (DTA/TG). The results showed that the catalyst obtained from combination of red mud with tannery shavings mixed in high ratio followed by thermal treatment and the unprocessed red mud were the most active. A 50% conversion in the range of 320–380 °C was achieved. In comparison, the other wastes showed lower activity, requiring much higher temperatures for the same conversion.

In view of the low cost involved and easy availability of such materials, their utilization as a source of catalyst can be of interest.

1. Introduction

Wastes originating from various industries are high in metal and metal oxide content and therefore have potential to be used as low cost catalysts. Simple physical and mechanical techniques may be employed to enhance the activity of the material without adding extra cost. Catalytic conversions of certain environmental pollutants like volatile organic compounds (VOCs) are carried over the oxides of transition metals like copper, iron and chromium [1]. Noble metal [2–4] based catalysts are very active for the hydrocarbon total oxidation, however their cost and stability against poisoning by sulfur and halides is an issue. Oxides of transition metals such as Fe, Cr, Mn, Ni, Cu and Co are also active for this reaction and are cheaper [5–9].

The wastes originating from industries like the tannery industry, the electroplating industry and the aluminium industry are high in their transition metal content either due to the raw material or processing and therefore have potential to be used as a source of catalytic materials for such reactions [10–13]. They are free of charge and their activity could be similar to that of mixed metal oxide catalysts prepared from fine chemicals.

Red mud is a by-product of the aluminium industry and has a high percentage of iron oxide. The other components present

include oxides of Al, Si, Ti, Ca, Na and others [14–16]. Due to its high alkalinity, it is considered an environmental hazard and requires special disposal methods [17]. Due to its high iron oxide content, there have been various studies testing the potential of red mud as a catalyst [12,18–20]. Red mud in addition to being used as a catalyst also has potential to be used as a catalyst support material [21]. Wastes generated from the tannery industry are high in chromium content and also have a high organic fraction. After the dewatering, dehairing, cleaning and de-fleshing of the hides they are sent for tanning. After classification of the leather it is shaved to generate leather of a constant thickness. The extra shavings may contain about 50% of moisture and approximately 3–5 wt.% Cr content. In addition significant amounts of sodium and calcium may also be present stemming from the chemical treatments employed. The high organic load of the waste gives it a suitable porous structure desirable for a catalyst and the chromium content provides catalytic activity [1]. Tanning of leather is performed with basic chromium sulfate, therefore the chromium in these solid wastes is generally present in the non-toxic +3 oxidation state however it may convert to the toxic state [22] therefore their release in the environment without proper treatment can lead to serious repercussions [23–25]. There have been a few studies on the use of chromium derived from waste material as catalyst [1,25]. Electroplating sludge is generated as a result of the precipitation of the heavy metals from the acidic/alkaline solutions and rinse water generated by electroplating processes. It is a complex solid mixture composed of multiple metals such as copper, zinc, chromium, iron
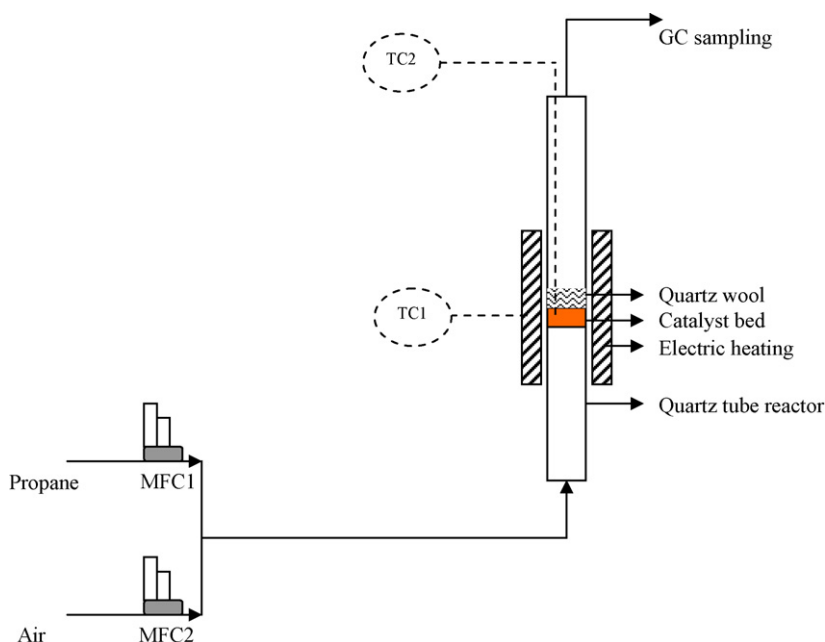
Fig. 1. Scheme for experimental set-up (TC1: thermocouple 1; TC2: thermocouple 2; MFC 1: mass flow controller for propane; MFC 2: mass flow controller for air).

and others. The wastes generated from the electroplating industry cause serious environmental problems due to the presence of a large amount of heavy metals and is considered a hazardous waste [26,27].

The present investigation aims at assessing the potential of utilizing industrial solid wastes such as red mud (RM), tannery shavings (TS) and electroplating sludge (EP) as sources of catalysts for oxidation reactions. The enhancement of catalytic activity of red mud can be achieved by addition of other active components like chromium, copper and nickel oxides. Propane was chosen as a model compound for this study and its total oxidation was examined. Propane is a cheap and stable compound which is easily available and is suitable for VOC combustion studies. The study employs simple thermal and mechanical treatments for processing the waste in an attempt to enhance the catalytic activity of the materials. Reactions were carried out at constant pressure and flow rates in a fixed bed reactor. Characterization of the catalysts was performed using various analytical techniques.

2. Experimental

2.1. Materials

The main material of interest in the investigation was red mud (RM). Three red mud samples were collected from different aluminium companies in India. They were in the form of dry powders with agglomerates. RM4 and RM7 were collected from a site in Tamil Nadu, India with a separation of two years while RM6 tailings were collected from a site in Jharkhand, India. All red mud samples were crushed, dried in an oven and then sieved ≤150 μm size.

The tannery shavings (TS) used in the propane oxidation reaction were collected from a tannery company located in Rehau, Southeastern Germany. The collected sample was dried at 110 °C for 24 h prior to analysis. The as received sample was in solid form with high moisture content.

The electroplating sludge from two different batches (EPI, EPII) was collected from an electroplating company located in Delhi, India. They were collected in pre-dried solid form from the company. No treatment was carried out on the sludge.

2.2. Catalyst preparation

2.2.1. Calcined red mud (CRM)

For calcination, the red mud samples were placed in silica crucibles and heated at a rate of 10 °C min^{-1} in static air to 550 °C and held for 4 h. The calcined samples show a colour change to bright red, indicating a phase change. The calcined samples were denoted as CRM.

2.2.2. Red mud and tannery shavings (RMTS)

The red mud samples were mechanically mixed with the tannery shavings in weight ratios of 1:1, 1:3 and 1:6 with a target Cr_2O_3 loading of 2%, 5% and 10%, respectively. The mixing was performed using a manual grinder and the samples were kept for calcination in static air at a temperature of 550 °C using a heating rate of 10 °C min^{-1} and duration of 4 h. The samples were referred to as RMTS.

2.2.3. Metal loaded red mud (MRM)

To load metal from electroplating sludge on red mud, the metal content was extracted using glacial acetic acid. For the extraction, 50 g of the sludge was taken in a flask, mixed with 200 ml glacial acetic acid and boiled at 120 °C for 2 h. This was followed by Soxhlet extraction for 8 h. The residue was dried and weighed. The mass loss in the case of EPI and EPII was 9 g and 16 g, respectively. The volume of the extracted liquid from the two sludges was mixed to get a high metal content in the final solution.

Simple mechanical mixing followed by calcination of red mud and electroplating sludge was not carried out since it does not give a homogeneous material. Instead, the extraction of metals was performed from the electroplating sludge and used for the impregnation of red mud.

For MRM (1), 12 g of red mud was taken in a round bottom flask and 60 ml of the mixed solution was added to it. This mixture was vacuum dried using *vaccubrand PC2001 VARI0 CVC 2000* while revolving at 100 RPM and temperature of 50 °C. The dried material was calcined in static air at a temperature of 550 °C for 4 h using a heating rate of 10 °C min^{-1}. MRM (2) with higher loading was prepared with 10 g of red mud and around 145 ml of mixed solution.

Table 1
Symbols used for the tested samples.

RM	'As-received' red mud
CRM	Calcined red mud
TS	Tannery shavings
CTS	Calcined tannery shavings
1:1 RMTS	Red mud mixed with tannery shavings in weight ratio of 1:1
1:3 RMTS	Red mud mixed with tannery shavings in weight ratio of 1:3
1:6 RMTS	Red mud mixed with tannery shavings in weight ratio of 1:6
MRM	Metals extracted from electroplating sludge impregnated on red mud

The 'as-received' red mud (RM) and calcined tannery shavings (CTS) were also tested for the total oxidation of propane under similar conditions for comparison. Table 1 provides a list of the symbols used for the characterized and tested samples.

2.3. Catalyst characterization

The composition of the starting materials red mud (RM) and tannery shavings (TS) were analyzed using inductively coupled plasma optical emission spectroscopy (ICP-OES) and atomic absorption spectroscopy (AAS), respectively. ICP-OES was performed using a Varian ICP Vista MPX model ICPAES radial and with a Varian Liberty 150 instrument. AAS was done by AAS 5EA and AAS 5FL by Analytik Jena. Samples were investigated as known masses of fine powders dissolved in mixed acids, with any insoluble portions having been given fusion treatment. Simultaneous analysis against known standards was performed.

The composition of the electroplating sludge was analyzed using X-ray fluorescence (XRF) spectroscopy using a Philips PW 2400 instrument. The extracted mixed solution from the electroplating sludge was analyzed using the ICP-OES technique.

The thermal analysis of the red mud samples was carried out on a DTA-TG apparatus, DTG-60 Shimadzu, in air. The analysis was carried out from 30 to 800 °C at a heating rate of 10 °C min^{-1}. Thermal analysis of tannery shavings was also carried out under similar conditions. The BET surface area of the samples was determined using the SMART Instrument model 92/93 using N_2 adsorption at liquid nitrogen temperature (−196 °C).

The phase analysis was undertaken by X-ray diffraction on a Bruker 08 X-ray diffractometer. The diffraction angle was swept from 10° to 80°. The 2θ scan range was covered with a step size of 0.02°. Some samples were also analyzed with a Philips X'Pert Pro X-ray diffraction system operating in reflection mode, with Co Kα_1 (λ = 1.78897 Å) radiation selected with a focusing monochromator, a symmetrically cut curved Johansson Ge$_{(1 1 1)}$ crystal, and a Philips X'celerator detector. A 2θ range from 10° to 100° was scanned in continuous mode. Identification of phases was accomplished by comparison with internationally recognized reference patterns JCPDS file.

The RM7 and MRM7 samples were examined by SEM using Leo Gemini 1530 SEM equipped with an INCA EDX system (Oxford Instruments). For the preparation of the samples the powder was
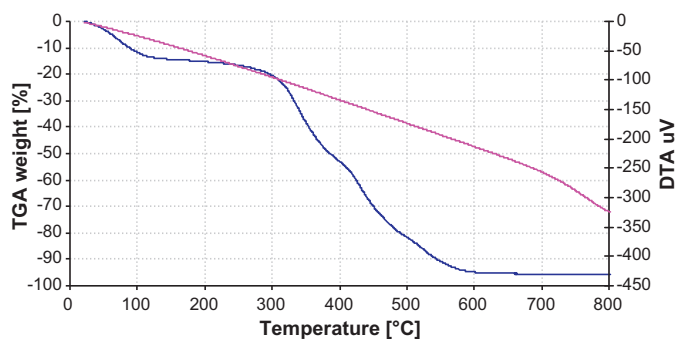

Fig. 2. TGA/DTA (heating rate 10 °C/min) of tannery shavings (TS).

Table 3
Chemical composition of tannery shavings samples (wt.% by ICP-OES).

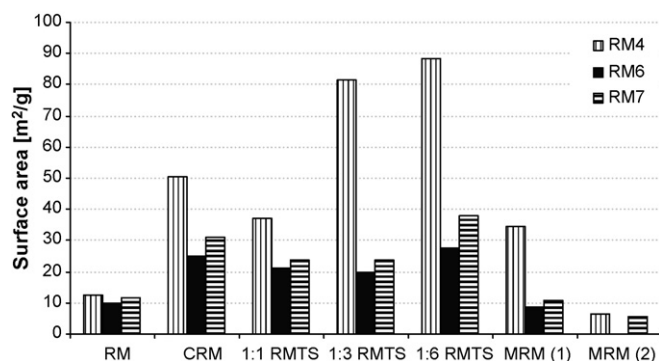|	
SiO_2	0.41
Al_2O_3	0.20
Fe_2O_3	0.08
CaO	0.11
MgO	0.06
Na_2O	0.23
K_2O	0.12
SO_3	0.21
Cr_2O_3	1.75
LOI[a]	96.80

[a] LOI: loss on ignition.

Fig. 3. BET surface area of different red mud samples.

embedded in epoxy resin and polished, followed by carbon coating in order to prevent charging of the sample by the electron beam. An accelerating voltage of 15 keV was used and images were recorded in backscattered electron mode.

2.4. Reaction studies

Fig. 1 shows the experimental setup used in the reaction study. The catalytic activity of the samples was determined in an electrically heated quartz tube-fixed bed reactor having an inner diameter of 1.8 cm. The catalyst was placed centrally in the reactor supported between a porous quartz disc and quartz wool plug. The temper-
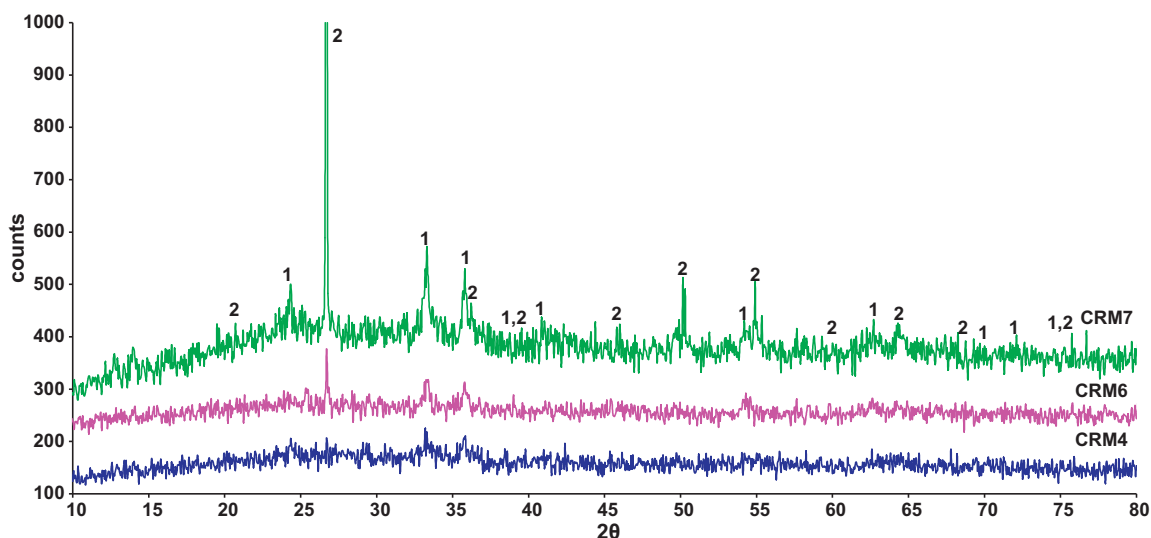
Table 2
Chemical composition of red mud samples (wt.% by ICP-OES).

Sample code	Major elements										
	SiO_2	Al_2O_3	Fe_2O_3	TiO_2	CaO	MgO	Na_2O	K_2O	P_2O_5	Cr_2O_3	LOI[a]
RM4	16.40	10.44	42.70	6.44	2.85	1.56	3.72	0.05	0.02	–	15.30
RM6	12.40	10.12	36.40	18.70	2.65	2.52	3.85	0.09	0.02	–	12.80
RM7	14.60	23.51	36.79	0.74	1.18	0.07	6.08	0.02	0.15	–	16.47

[a] LOI: loss on ignition.

Fig. 4. XRD pattern of calcined red mud (1: hematite: 33-0664; 2: quartz: 46-1045).

atures were measured at two points, one just outside the reactor and the second directly in the catalyst bed. A NiCr–Ni thermocouple was employed for the purpose.

The gas distribution system was made of stainless steel and MFCs (Brooks smart mass flow 5850 s) were used to maintain the flow rate of the gases. A pressure release system was used to maintain the pressure of the gas distribution system around 1.1 bar. A feed gas mixture of 5000 ppmv propane in air was used for the reaction. A flow rate of 10 l/h was employed giving a GHSV of 5000 h^{-1}. The product gas mixture was analyzed in a Hewlett Packard 5890 series II GC fitted with TCD and Poraplot Q column of 30 m length and 0.32 mm diameter. Samples of the outlet gas were taken and analyzed every 8 min. Background experiments were performed using an empty reactor tube containing quartz wool plugs only. It was observed that below 600 °C there was negligible contribution of the reactor/temperature on propane oxidation. The conversion was calculated from the propane concentration in the inlet and outlet streams.

3. Results and discussions

3.1. Material characterization

Table 2 shows the composition of the various red mud (RM) samples. Fe_2O_3 is the major component in all the red mud samples. The other major components present include SiO_2, Al_2O_3 and TiO_2. The difference in the composition of red mud reflects the differences in the original ore, the processing and/or the post generation additions. While Fe imparts the main catalytic activity, components such as Na and Ti may influence the behaviour of the material [28]. Table 3 provides the chemical composition of the tannery shavings (TS) which were mixed with red mud for the RMTS samples. Cr_2O_3 has the highest concentration of 1.75% by weight. Na_2O is also present in considerable amounts, which may be due to the use of chemicals such as sodium chloride, during the processing of the hides. The tannery shavings have a very high LOI (loss on ignition) value of 96.8% since bulk of it is made of organic matter. Thermal analysis conducted on tannery shavings showed a similar result with a mass loss of more than 90% (Fig. 2).

Table 4 provides the composition of the electroplating sludges (EP) I and II. The major constituents of the EP sludge were SiO_2, Al_2O_3, Fe_2O_3, CaO and Na_2O while in terms of heavy metals high

amounts of chromium, zinc, nickel and copper were present. The value of the metals in the extracted mixed solution is provided in Table 5. Chromium has the highest concentration of 4078 mg/l followed by zinc and nickel.

Table 4
Composition of waste from the electroplating industry (wt.% by XRF and ICP-OES).

Probe name	EP I	EP II
wt.%		
SiO_2	68.27	48.98
TiO_2	0.28	0.22
Al_2O_3	7.47	6.13
Fe_2O_3	2.87	2.80
MnO	0.05	0.08
MgO	2.12	2.32
CaO	3.33	4.23
Na_2O	3.79	12.94
K_2O	1.56	1.65
P_2O_5	0.36	1.90
SO_3	0.91	2.80
Total	90.10	81.25
LOI	4.74	7.55
ppm		
V	54	46
Cr	36,689	45,336
Co	16	360
Ni	5309	46,703
Cu	4799	10,847
Zn	33,715	60,348
Rb	124	123
Sr	481	839
Y	24	26
Zr	229	293
Nb	12	17
Ba	340	329
Pb	167	166
U	<n.d.	<n.d.
S	15,894	22,753
Cl	4096	17,067

Table 5
Composition of extracted mixed solution from electroplating sludge (mg/l by ICP-OES).

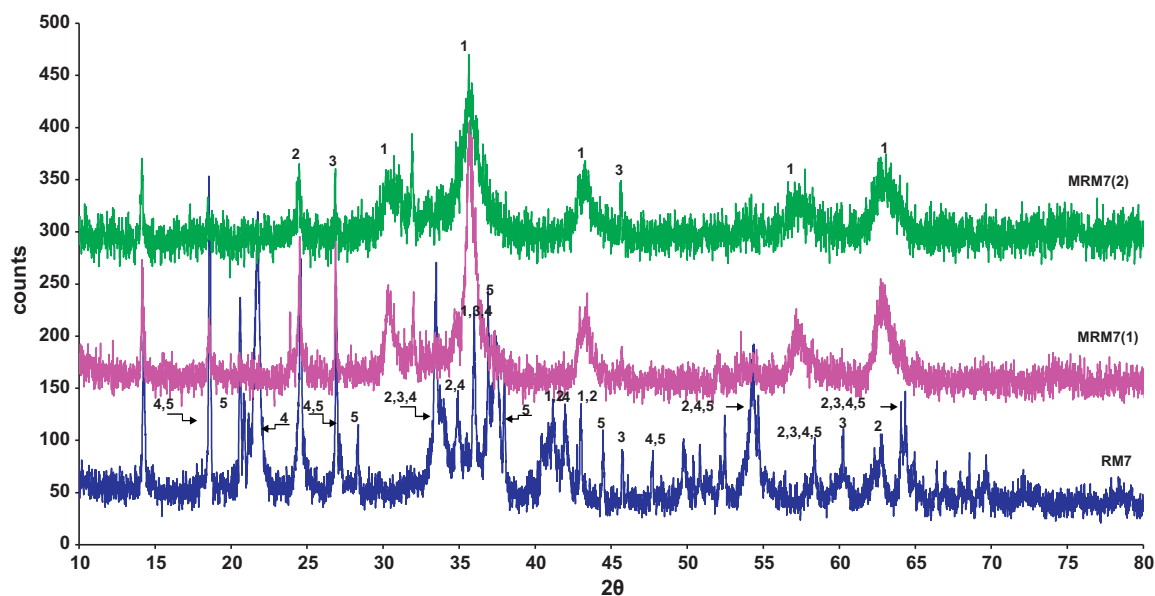|	
Co	25
Cr	4078
Cu	384
Ni	2539
Zn	2677

Fig. 5. XRD pattern for MRM7 (1), MRM7 (2) and RM7 (1: magnetite: 19-0629; 2: hematite: 33-0664; 3: quartz: 46-1045; 4: goethite: 29-0713; 5: gibbsite: 33-0018).

The specific surface area of the as-received red mud (RM), calcined red mud (CRM), red mud mixed with tannery shavings (RMTS) and loaded red mud (MRM) are provided in Fig. 3. The surface area of as-received red mud for all the samples is similar, lying in the range of 10–13 m^2/g. In the case of treatments like calcination and mechanical mixing of red mud with tannery shavings the increase in surface area of RM6 and RM7 is marginal and similar, however in all the cases the surface area of red mud involving RM4 is substantially higher than its counterparts. In case of metal loaded red mud (MRM) the surface area of all the samples except MRM4 (1) are reduced drastically, indicating sintering of the samples. The increase in surface area of the red mud samples upon calcination is a known factor and is the result of phase changes induced by dehydration of iron and aluminium hydroxides during heating of the sample [29,30].

The XRD scan of the as-received red mud (RM), reported previously [20] revealed that the main iron-bearing phases in all the samples were goethite and hematite. Al was present as boehmite (AlO(OH)) or gibbsite (Al(OH)$_3$) and Si as quartz and minor mixed silicates. Anatase (TiO$_2$) was a component in RM6. The main phases in the calcined red mud (CRM) were hematite and quartz in all the samples (Fig. 4). All the treated samples result in poorly or nano-crystalline phases making their identification by XRD difficult. The main components observed in MRM samples are magnetite (or maghemite) and quartz (Fig. 5). The magnetite peaks are broadened pointing to a nano-crystalline dehydration product. In MRM (2), iron chromium oxide, which has peaks similar to magnetite, could also be present. Quartz, hematite and magnetite were observed in RMTS samples. Similar to the MRM (1 and 2), iron chromium oxide is also observed in case of RMTS samples with high chromium content (e.g. 1:6 RMTS).

The TGA/DTA analysis of RM4, RM6 and RM7 are shown in Fig. 6. The thermal analysis conducted on red mud in various studies describes a three step weight loss. The initial weight loss corresponds to loss of the physically bonded water in red mud. The second major loss of weight takes place due to the loss of chemically bound water from goethite and gibbsite phase, this could range anywhere from 105 to 450 °C. Finally from 560 to 720 °C, the decomposition of calcite might take place [31]. Previous studies on red mud have reported gibbsite decomposition at temperatures of 271 °C, 287 °C [32] and 287.5 °C [33]. In this study, the main peak
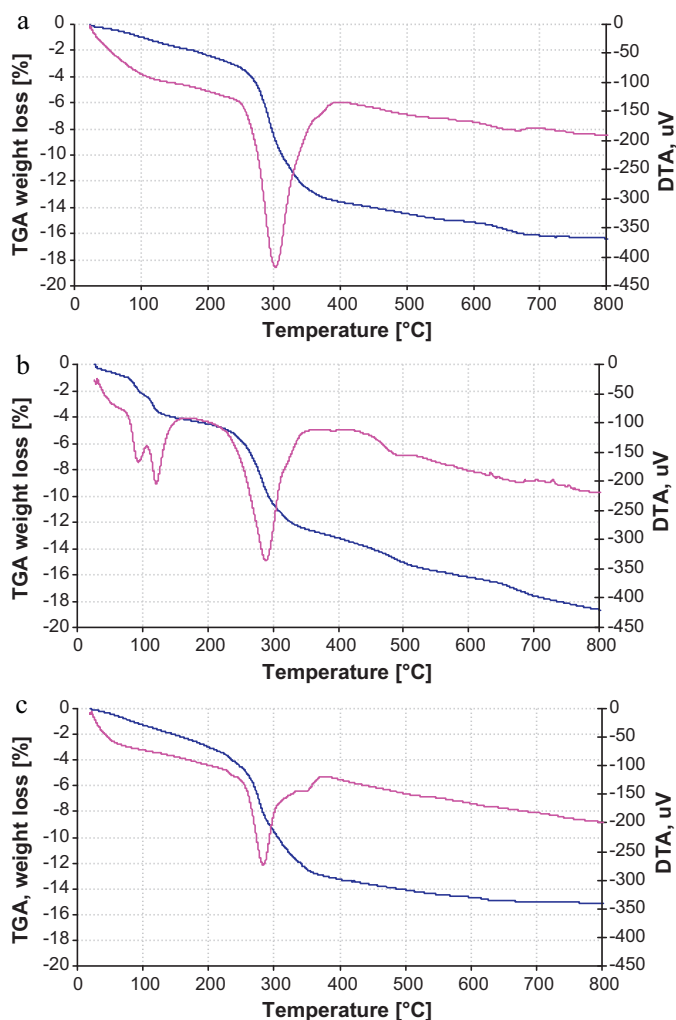

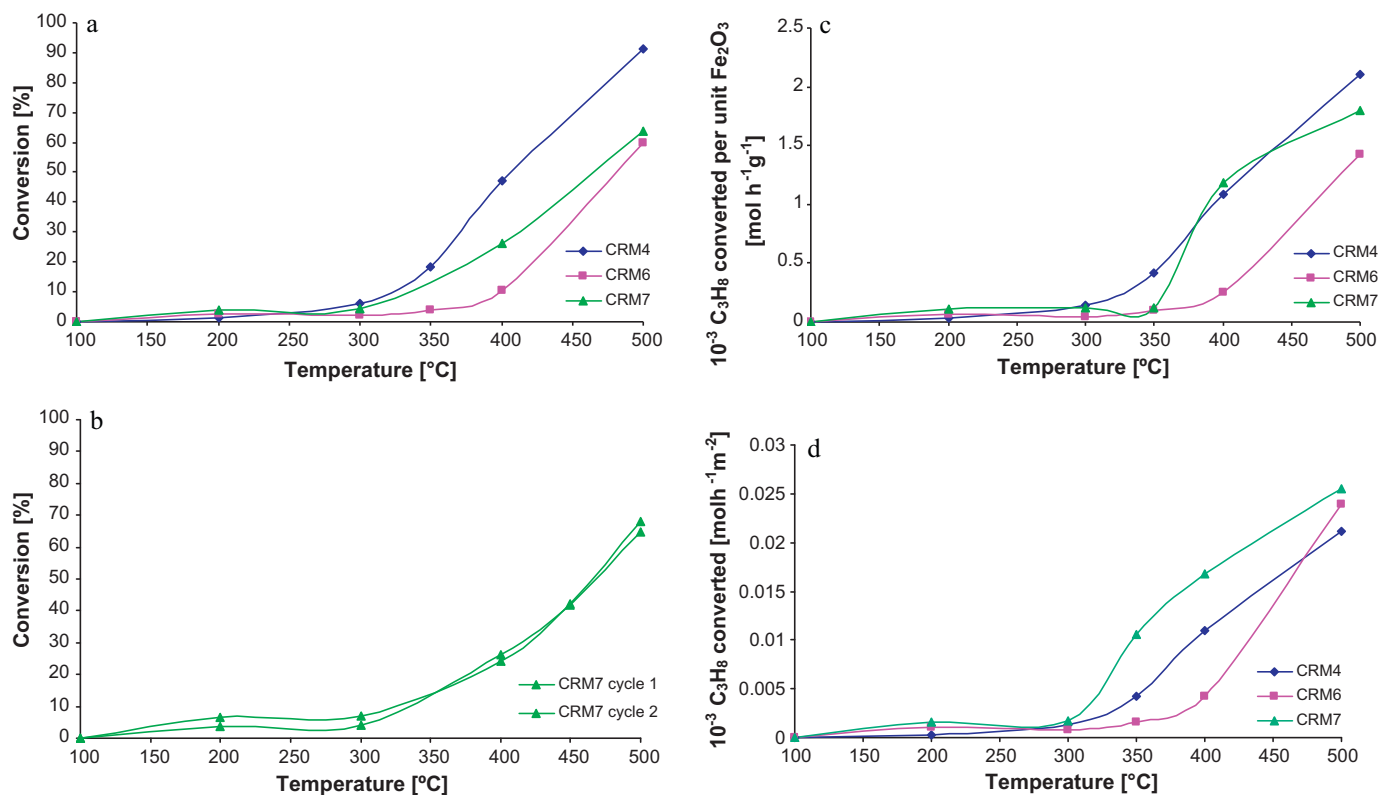**Fig. 6.** TGA/DTA (heating rate 10 °C/min) of (a) RM4, (b) RM6 and (c) RM7.

Fig. 7. Conversion of propane (0.5% C_3H_8 in air, GHSV 5000 h^{-1}, 2.0 cm^3 catalyst) over (a) calcined red mud, (b) CRM7 cycle 1 and 2 conversion. Rate of propane converted over CRM (c) per gram Fe_2O_3 and (d) per m^2 surface area.

in all samples occurs from the range 290 to 300 °C and the main weight loss takes place between 200 and 400 °C which could correspond to the loss of water from goethite and gibbsite phases [32]. RM6 shows extra peaks around 90 °C and 110 °C. The total weight loss observed in case of RM4, RM6 and RM7 till 800 °C was 16%, 18% and 14%, respectively. While the weight seems to stabilize in case of RM4 and RM7 after reaching a temperature of 800 °C, in case of RM6 it seems to be decreasing further. The DTA curve did not show any peaks beyond 400 °C.

3.2. Reaction study results

Fig. 7a shows the propane conversion over CRM4, CRM6 and CRM7. The reaction products observed in all cases were carbon dioxide and water. CRM4 shows the highest conversion of 90% at 500 °C, while CRM6 gives the lowest activity. The final conversion of CRM6 and CRM7 at 500 °C reaches 60%. 50% conversion was obtained in the range 400 to 500 °C. To check the stability of the calcined red mud the propane conversion was tested over CRM7 by repeating the reaction cycle with the same catalyst. The performance on CRM 7 in both cycles was found to be comparable (Fig. 7b). To understand the contribution of the expected catalytically active phase, Fe_2O_3, the rates were plotted per gram active phase and per m^2 of surface area. Other phases such as TiO_2 may contribute towards the reaction while Na_2O may have a sintering effect; however, the influence of iron phases is expected to be maximum and is therefore considered. Fig. 7(c) and (d) shows the rate of propane converted over CRM per gram Fe_2O_3 and per m^2 surface area. From the figure it is seen that the performance of CRM4 and CRM7 is similar in case of rate of propane converted per gram Fe_2O_3. This indicates that in addition to the iron content, surface area is also an important factor influencing the activity of the material. Due to the higher Fe_2O_3 content of CRM4, its activity per m^2

surface area is expected to be higher, however from the plot we observe that CRM7 shows a higher activity than CRM4. The possible reason could be that not all iron species are active sites for the reaction. In addition some non-controllable elements present in these materials may also be contributing to the catalytic activity. CRM6 shows a lower rate compared to CRM4 and CRM7. It must be pointed out that no significant loss of surface area was observed in the samples as a function of the increasing reaction temperature.

The activity of RMTS was found to be better than that of CRM. The addition of tannery shavings to red mud followed by calcination increased the activity proportionally to the increasing ratio of tannery shavings to red mud. The conversion of propane over 1:1, 1:3 and 1:6 RMTS can be observed in Fig. 8. This is attributed to the contribution of chromium oxide from tannery shavings.

In this case as well, the activity is in the order of RM4TS > RM7TS > RM6TS, similar to calcined red mud. 1:6 RM4TS reaches almost complete oxidation around 350 °C.

For comparison as-received red mud (RM) and calcined tannery shavings (CTS) were also studied. The calcination conditions used for tannery shavings were similar to those used for calcined red mud. Fig. 9a depicts the conversion of propane over 'as received' red mud samples. The performance of all the samples is found to be similar. The 50% conversion for all the samples lies in the range of 350–370 °C. A run with RM7 with similar conditions of temperature programmed temperature increase, maintained at 500 °C till 4000 min time on stream showed a stable activity of the catalyst. However, the performance of as-received red mud is reduced in the second cycle and is similar to CRM7 (Fig. 9b). The higher activity in the first cycle could be attributed to the presence of FeOOH (goethite) which changes in situ to Fe_2O_3 (hematite) in the first run as observed in the thermal analysis and is not available in the subsequent cycles. A similar phenomenon was observed by Li et al.
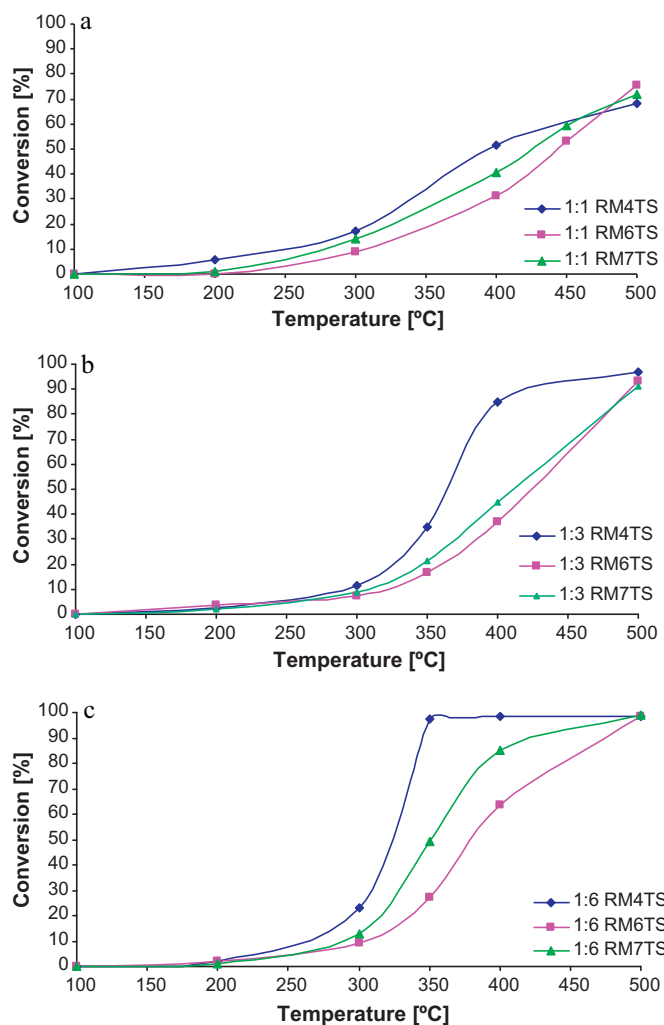
Fig. 8. Conversion of propane (0.5% C_3H_8 in air, GHSV 5000 h^{-1}, 2.0 cm^3 catalyst) over (a) 1:1RMTS, (b) 1:3RMTS, and (c) 1:6RMTS.
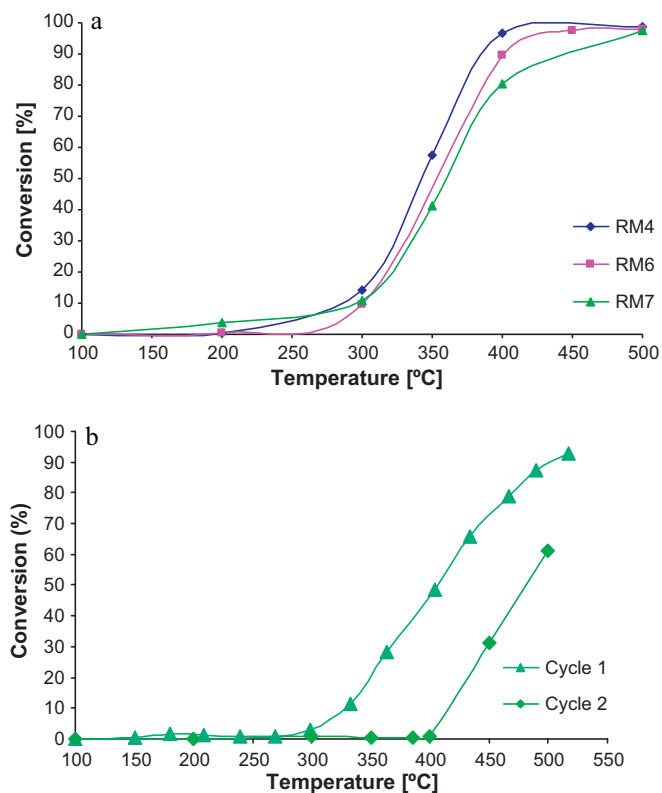

Fig. 9. Conversion of propane (0.5% C_3H_8 in air, GHSV 5000 h^{-1}, 2.0 cm^3 catalyst) over (a) untreated red mud and (b) RM7 cycles 1 and 2.

[34] during the oxidation of carbon monoxide over a commercial iron oxide catalyst containing both iron oxide and iron hydroxide. The reason for the higher activity of FeOOH over Fe_2O_3 is the relative ease with which it loses the oxygen. The Fe–O bond length in case of FeOOH is longer (2.103 Å) than Fe_2O_3 (2.08 Å) and hence the breaking of the Fe–O bond is easier [34]. Once the peak activity is reached in the first cycle, it is maintained over a long period.

The post reaction samples of as-received and calcined red mud were similar. Both contained hematite and quartz as the major
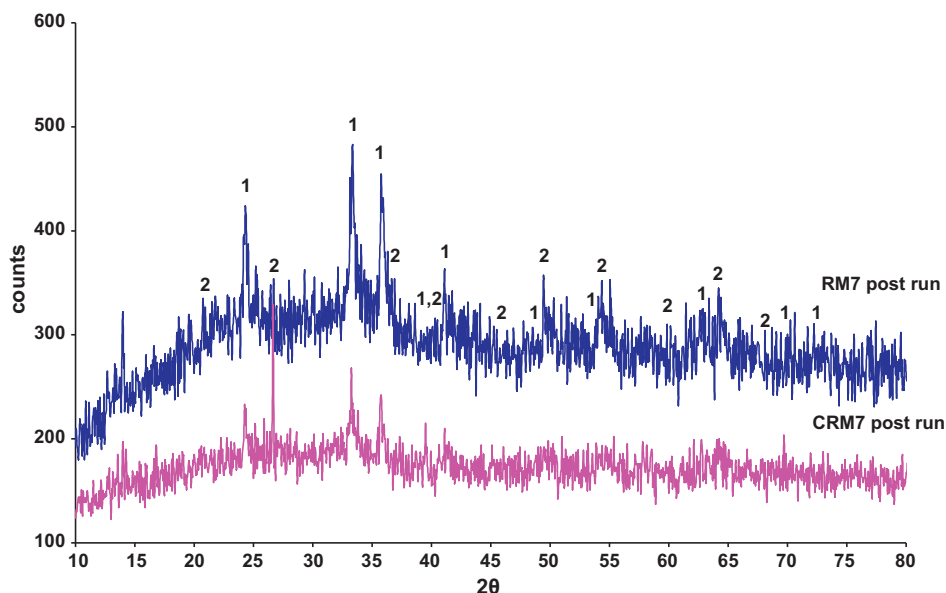

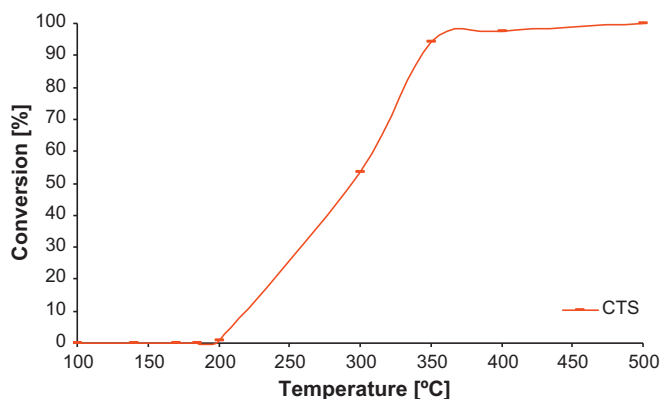**Fig. 10.** XRD pattern of post run RM7 and CRM7 samples (1: hematite: 33-0664; 2: quartz: 46-1045).

Fig. 11. Conversion of propane (0.5% C_3H_8 in air, GHSV 5000 h^{-1}, 2.0 cm^3 catalyst) over CTS.

phases and were more amorphous compared to their pre-reaction samples. Quartz peaks were more noticeable in case of CRM7 (Fig. 10).

Calcined tannery shavings (CTS) were the most active material for the reaction, however due to its very fine size it is not possible to go to higher GHSV. The 50% conversion was obtained around 290 °C, while total oxidation was obtained near 365 °C. It is noteworthy that above 350 °C, the performance of CTS and 1:6RM4TS were comparable (Fig. 11). In addition, in contrast to CTS, RMTS appeared more suitable for high GHSVs.

In the case of RMTS, the expected rates from individual contributions of Fe_2O_3 and Cr_2O_3 obtained from CRM and CTS, respectively, were compared with the actual rates obtained. It was found that the expected rates were higher than the actual rates obtained. For example in case of 1:6RM7TS the expected rate at 500 °C is 3.51×10^{-3} mol C_3H_8 converted/h-g catalyst, while the actual rate is 2.00×10^{-3} mol C_3H_8 converted/h-g catalyst. The difference was found to increase with the increase in the reaction temperature. The difference in the theoretical and actual rates is expected since the Fe_2O_3 and Cr_2O_3 are not present in isolation and could have formed mixed iron–chromium oxides as observed by XRD analysis.

The samples prepared by loading of extracted metals of electroplating sludge onto red mud, gave a higher activity than the 1:1 RMTS in terms of final conversion at 500 °C, however in terms of the light off temperature it was lower than all the RMTS (Fig. 12). The conversion on MRM6 does not even reach >90% unlike the other MRM samples. A look at the surface area suggests that the impregnation process followed by calcination led to sintering and caused a decrease in the activity. Using the two better performing MRM4 and MRM7, the tests were repeated with a higher loading (termed as MRM (2)). The results however revealed that the activity was
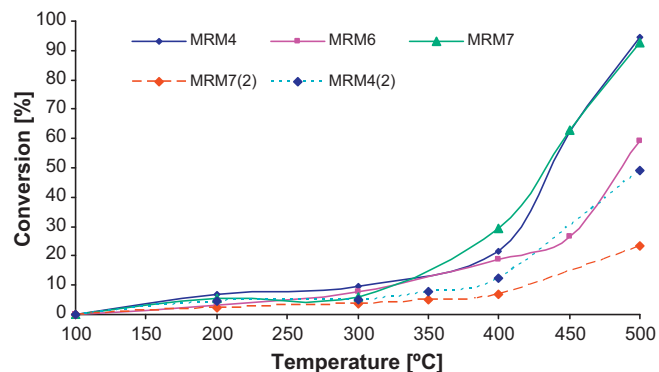

Fig. 12. Conversion of propane over MRM (1) and MRM (2) (0.5% C_3H_8 in air, GHSV 5000 h^{-1}, 2.0 cm^3 catalyst).
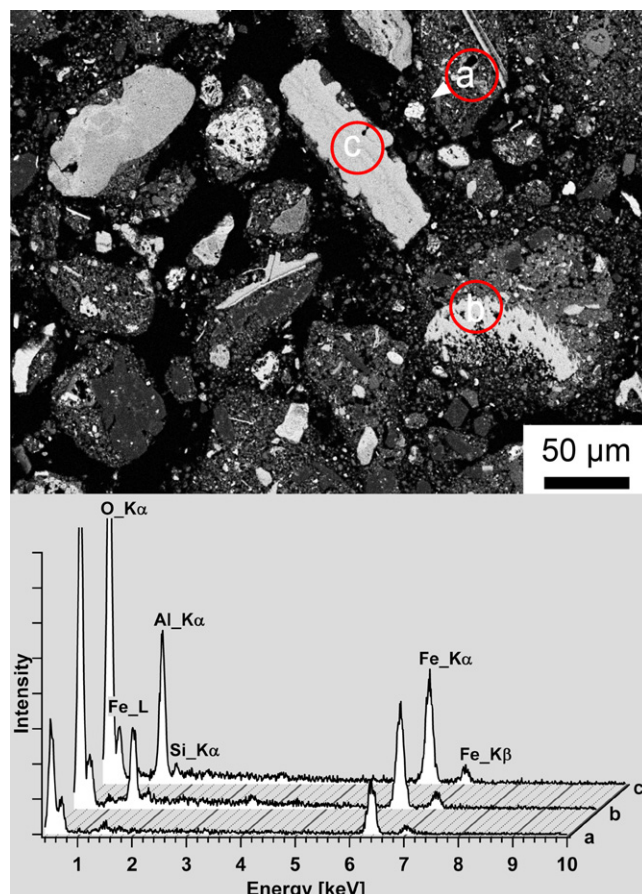

Fig. 13. Backscattered electron image and EDX analyses of RM7. Iron (hydr)oxides in the untreated red mud vary in grain size, texture and composition.

drastically reduced. The surface area of the MRM samples suggests sintering post impregnation and heating process which limits the contact of the reactant gases with the catalyst surface and therefore causes a drastic reduction in the activity. SEM-EDX analysis was conducted for RM7 and MRM7 (1 and 2), in order to compare them.

In RM7 main phases of iron and aluminium were present and a large variation was observed in terms of composition, grain size and texture of the iron oxides (Fig. 13). Large differences in Al content of the iron oxides are attributed to the different solubility of Al in goethite and hematite. In goethite, up to one third of Fe can be replaced by Al while hematite can accommodate up to one sixth of Al [30].

In MRM7 (2) samples all iron oxides show a low Cr content together with some Na, Al and Ca. In contrast to the RM sample small grains with a grain size of 200 nm to 1 μm were frequently found. These small grains are mostly associated with the metals of the electroplating waste and show high content of Cr, Ni and Zn (Fig. 14). The composition varies strongly from grain to grain. Some show almost equal amounts of Cr and Fe while other are composed of variable amounts of Fe, Cr, Ni and Zn. A few grains were found that contained mainly Ni with minor Fe. Most of the small grains were also found to be associated with Cl$^-$. However, many grains are smaller than the volume X-rays are generated from and thus the EDX spectra give a sum signal from the grains and their surroundings. However, they seem to concentrate most of the transition metals.

Therefore, the dispersion of the metals is not uniform over the catalytically active iron oxides as intended which could also contribute to the low activity.
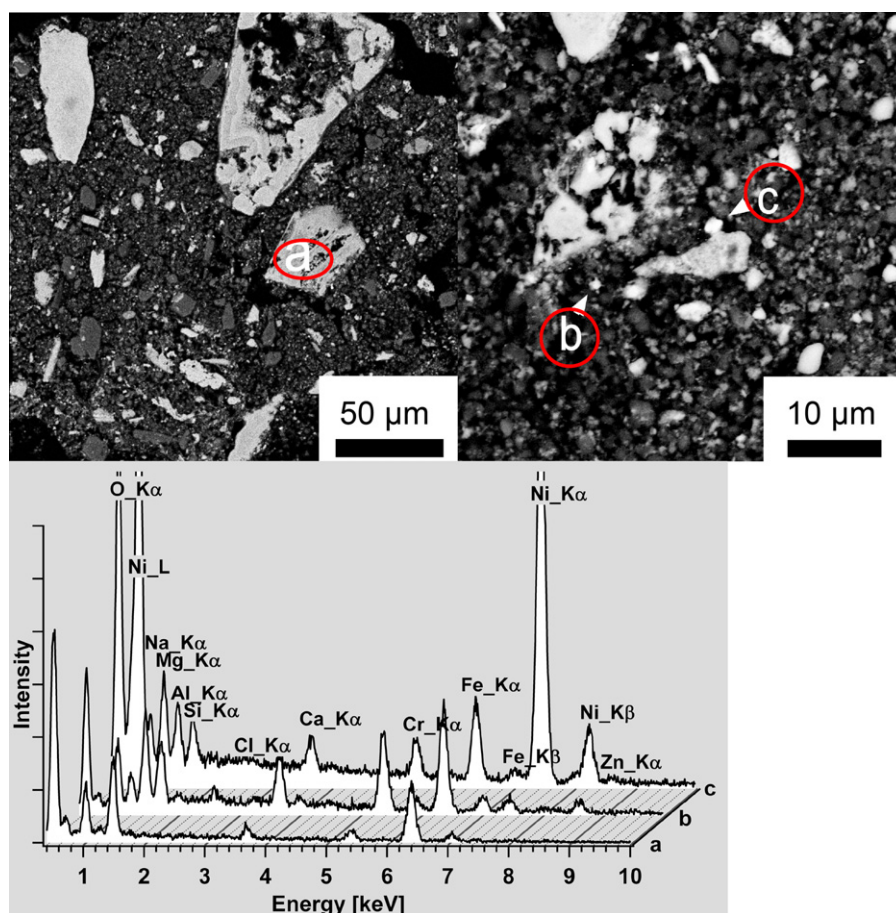
Fig. 14. Backscattered electron images and EDX analyses of MRM7 (2). The Cr and Ni content of iron oxide depend strongly on grain size. Larger grains show a low Cr content while small grains (<2 μm) give significant EDX signals.

Since the XRD patterns of RMTS and MRM samples are similar, there seem to be other factors influencing the activity as well. The concentration of metals present in MRM and RMTS samples determined by ICP-OES is shown in Fig. 15. The amount of Cr present in MRM7 (2) and 1:6RM7TS is very similar (5.8% and 5.9%, respectively). In addition, MRM7 (2) also has 3.3% Zn, 1.9% Ni, 0.6% Cu and 0.02% Co. Another notable factor is the high amount of Na present in both MRM samples. This could explain the low surface area observed in case of the MRM samples where in addition to the pore clogging, the sodium present could be acting as a sintering aid [28]. However, the removal of sodium can be achieved by simple methods such as washing with water or by digestion with HCl followed by reprecipitation [28].

It must be pointed out that the performance of the studied materials is lower in comparison to the commercial catalysts when compared in terms of feed composition and flow rate conditions; however, the study shows the feasibility of using such waste materials as a source of catalyst for VOC oxidation. Klose et al. [1] tested a commercial catalyst CC-4 for the total oxidation of propane under similar conditions as the present study but with a GHSV of 10,000 h^{-1}. The catalyst consisted of Al$_2$O$_3$ as the support (71 wt.%) and Fe$_2$O$_3$ as the active component (21 wt.%). Under these conditions the catalyst was able to achieve a 50% conversion at 500 °C. The best performance of the commercial catalyst was by CC-1 which consisted of Co$_3$O$_4$ (18.9 wt.%) and MnO$_2$ (9.1 wt.%) as the main active component supported on La$_2$O$_3$ (68 wt.%) and Sr$_2$O$_3$ (4.1 wt.%). The 50% conversion in this case was achieved at 330 °C. Solsona et al. [5] tested alumina supported Co$_3$O$_4$ (20 wt.%) for total oxidation of propane using 250 mg catalyst and a feed composition of 8000 ppmv at a flow rate of 50 ml/min; the 50% conversion was obtained at 360 °C. Another catalyst, CO-100 (Co$_3$O$_4$ 100 wt.%) tested by them under the same conditions gave a 50% conversion at 235 °C. The same authors [6] investigated mesoporous Co$_3$O$_4$ made from silica based hard templates and cobalt nitrate. Propane testing was done using 250 mg catalyst, 8000 vppm propane in air feed composition and a flow rate of 50 ml min^{-1}. Total conversion of propane was reached at temperatures between 225 and 250 °C. Nanocrystalline Co$_3$O$_4$ prepared by three different methods were tested by Cao et al., for propane conversion using a feed composition of 1 vol% propane and a flow rate of 100 ml min^{-1}. The highest activity was observed for Co$_3$O$_4$ prepared by soft reaction grinding based on citrate precursor which achieved total conversion at
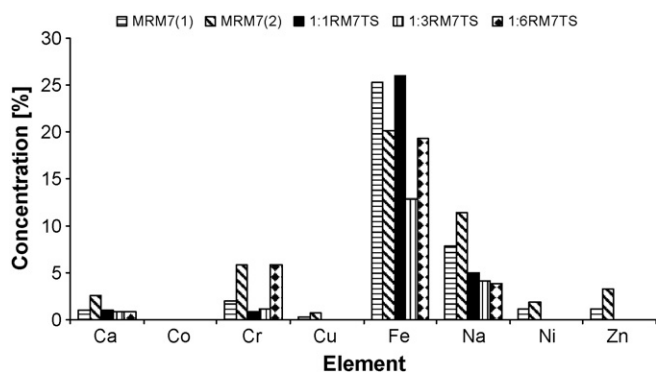

Fig. 15. Bar graph showing element concentration in MRM and RMTS (by ICP-OES).

240 °C [35]. Balahwane and coworkers [7] tested Co_3O_4 deposited on cordierite monolith using chemical vapour deposition using a feed containing 3000 vppm propane at a flow rate of 500 sccm. Total conversion of propane was achieved at 475 °C. Co_3O_4 catalysts on different supports (titania, ceria, alumina) were tested by Lamonier and coworkers [8] for deep oxidation of propene. The highest activity was observed for ceria support with total conversion at 275 °C.

Pt catalysts have been examined on different supports for VOC oxidation. Stakheev and coworkers [3] determined the activity of nanosized platinum catalysts supported on alumina using a feed containing 5000 vppm propane in air and GHSV 60,000 h^{-1}. At 280 °C, total oxidation of propane was observed. In another study on Pt supported on Al_2O_3, an inlet gas containing 10,000 vppm propane and space velocity 16,000 h^{-1} was used; total conversion was obtained at 400 °C [36]. Perez-Cadenas et al. [4] studied the catalytic behaviour of Pt catalysts supported on carbon-based monoliths against aromatic hydrocarbons. Carbon coating was done on a cordierite monolith by carbonizing polyfurfuryl alcohol. The catalyst (Pt) loading of 0.35–0.90% was obtained using nitrate impregnation. The best catalyst shows a total conversion of benzene at 155 °C.

4. Conclusion

The possibility of utilizing industrial waste materials for the VOC oxidation is depicted using propane as a model compound. The amount of active component present in the waste such as Fe_2O_3 in red mud and Cr_2O_3 in tannery shavings is an important factor in determining the activity of the sample. In all the treated samples, RM4 batch which had the highest Fe_2O_3 content and the highest surface area, gave the highest conversion. By adding chromium containing waste to red mud samples, the activity increased with the increasing proportion of tannery shavings and chromium oxide acts as the main catalytic component.

Despite a high metal concentration present in the MRM samples, its activity is low and decreased further with the increasing loading. The low surface area, high sodium content and presence of Cl$^-$ leads to its low activity.

Hematite in itself is not considered very active for propane oxidation; therefore the tests performed on the 'as-received' red mud indicated that the *in situ* transformation of the hydroxides to the oxides helps achieve a higher conversion at a lower temperature. However since no calcination is done on these samples, they are unstable and give a lower conversion in the second cycle of operation. This is similar to the performance of the calcined red mud.

Since the source of the catalysts employed here is industrial wastes, they are cheap and easily available.

References

[1] F. Klose, P. Scholz, G. Kreisel, B. Ondruschka, R. Kneise, U. Knopf, Catalysts from waste materials, Appl. Catal. B: Environ. 28 (2000) 209–221.

[2] A.C. Gluhoi, N. Bogdanchikova, B.E. Nieuwenhuys, Total oxidation of propene and propane over gold-copper oxide on alumina catalysts. Comparison with Pt/Al$_2$O$_3$, Catal. Today 113 (2006) 178–181.

[3] A.M. Gololobov, I.E. Bekk, G.O. Bragina, V.I. Zaikovskii, A.B. Ayupov, N.S. Telegina, V.I. Bukhtiyarov, A.Y. Stakheev, Platinum nanoparticle size effect on specific catalytic activity in *n*-alkane deep oxidation: dependence on the chain length of the paraffin, Kinet. Catal. 50 (2009) 830–836.

[4] A. Perez-Cadenas, S. Morales-Torres, F.J. Maldonado-Hodar, F. Carrasco-Marın, Carbon-based monoliths for the catalytic elimination of benzene, toluene and m-xylene, Appl. Catal. A: Gen. 366 (2009) 282–287.

[5] B. Solsona, T.E. Davies, T. Garcia, I. Vazquez, A. Dejoz, S.H. Taylor, Total oxidation of propane using nanocrystalline cobalt oxide and supported oxide catalysts, Appl. Catal. B: Environ. 84 (2008) 176–184.

[6] T. Garcia, S. Agouram, J.F. Sanchez-Royo, R. Murillo, A.M. Mastral, A. Aranda, I. Vazquez, A. Dejoz, B. Solsona, Deep oxidation of volatile organic compounds using ordered cobalt oxides prepared by a nanocasting route, Appl. Catal. A: Gen. 386 (2010) 16–27.

[7] Z. Tian, N. Bahlawane, F. Qi, K. Kohse-Höinghaus, Catalytic oxidation of hydrocarbons over Co$_3$O$_4$ catalyst prepared by CVD, Catal. Commun. 11 (2009) 118–122.

[8] F. Wyrwalski, J.-M. Giraudon, J.-F. Lamonier, Synergistic coupling of the redox properties of supports and cobalt oxide Co$_3$O$_4$ for the complete oxidation of volatile organic compounds, Catal. Lett. 137 (2010) 141–149.

[9] J.R. Paredes, E. Díez, F.V. Díez, S. Ordóñez, Combustion of methane in lean mixtures over bulk transition metal oxides: evaluation of the activity and self-deactivation, Energy Fuels 23 (2009) 86–93.

[10] O.E. Lebedeva, A.G. Sarmurzina, Industrial wastes as catalyst precursors: VOC oxidation, Appl. Catal. B: Environ. 26 (2000) L1–L3.

[11] R. Weber, K. Nagai, J. Nishina, H. Shiraishi, M. Ishida, T. Takasuga, K. Konndo, M. Hiraoka, Effects of selected metal oxides on the dechlorination and destruction of PCDD and PCDF, Chemosphere 46 (2002) 1247–1253.

[12] S. Sushil, V.S. Batra, Catalytic applications of red mud, an aluminium industry waste: a review, Appl. Catal. B: Environ. 81 (2008) 64–77.

[13] J.M. Lee, J.H. Kim, Y.Y. Chang, Y.S. Chang, Steel dust catalysis for fenton-like oxidation of polychlorinated dibenzo-p-dioxins, J. Hazard. Mater. 163 (2009) 222–230.

[14] J. Yang, B. Xiao, Development of unsintered construction materials from red mud wastes produced in the sintering alumina process, Construct. Build. Mater. 22 (2008) 2299–2307.

[15] S. Wang, H.M. Ang, M.O. Tadé, Novel applications of red mud as coagulant, adsorbent and catalyst for environmentally benign processes, Chemosphere 72 (2008) 1621–1635.

[16] Y. Pontikes, C. Rathossi, P. Nikolopoulos, G.N. Angelopoulos, D.D. Jayaseelan, W.E. Lee, Effect of firing temperature and atmosphere on sintering of ceramics made from Bayer process bauxite residue, Ceram. Int. 35 (2009) 401–407.

[17] W. Liu, J. Yang, B. Xiao, Application of Bayer red mud for iron recovery and building material production from alumosilicate residues, J. Hazard. Mater. 161 (2009) 474–478.

[18] S. Ordóñez, H. Sastre, F.V. Díez, Hydrodechlorination of tetrachloroethylene over modified red mud: deactivation studies and kinetics, Appl. Catal. B: Environ. 34 (2001) 213–226.

[19] J.R. Paredes, S. Ordóñez, A. Vega, F.V. Díez, Catalytic combustion of methane over red mud-based catalysts, Appl. Catal. B: Environ. 47 (2004) 37–45.

[20] M. Balakrishnan, V.S. Batra, J.S.J. Hargreaves, A. Monaghan, I.D. Pulford, J.L. Rico, S. Sushil, Hydrogen production from methane in the presence of red mud-making mud magnetic, Green Chem. 11 (2009) 42–47.

[21] K. Pirkanniemi, M. Sillanpää, Heterogeneous water phase catalysis as an environmental application: a review, Chemosphere 48 (2002) 1047–1060.

[22] S. Tahiri, A. Albizane, A. Messaoudi, M. Azzi, J. Bennazha, S.A. Younssi, M. Bouhria, Thermal behaviour of chrome shavings and of sludges recovered after digestion of tanned solid wastes with calcium hydroxide, Waste Manage. 27 (2007) 89–95.

[23] M. Erdem, Chromium recovery from chrome shaving generated in tanning process, J. Hazard. Mater. B129 (2006) 143–146.

[24] L.C.A. Oliveira, M.C. Guerreiro, M. Gonçalves, D.Q.L. Oliveira, L.C.M. Costa, Preparation of activated carbon from leather waste: a new material containing small particle of chromium oxide, Mater. Lett. 62 (2008) 3710–3712.

[25] F. Prinetto, G. Ghiotti, S.D. Rossi, G.D. Modica, CrOx/SiO$_2$ catalysts prepared using chromium recovered from tanning sewage, Appl. Catal. B: Environ. 14 (1997) 225–239.

[26] C. Li, F. Xie, Y. Ma, T. Chai, H. Li, Z. Huang, G. Yuan, Multiple heavy metals extraction and recovery from hazardous electroplating sludge waste via ultrasonically enhanced two stage acid leaching, J. Hazard. Mater. (2010), doi:10.1016/j.jhaz.2010.02.013.

[27] I. Dobrevsky, M. Dimova-Todorova, T. Panayotova, Electroplating rinse waste water treatment by ion exchange, Desalination 108 (1996) 277–280.

[28] K.C. Pratt, V. Christoverson, Hydrogenation of a model hydrogen-donor system, using activated red mud catalyst, Fuel 61 (1982) 460–462.

[29] US Patent, 50,51,243 (1991).

[30] R.M. Cornell, U. Schwertmann, The Iron Oxides: Structure, Properties, Reactions, Occurrences and Uses, 2nd ed., Wiley-VCH GmbH & Co. KG, 2003.

[31] Y. Liu, C. Lin, Y. Wu, Characterization of red mud derived from a combined Bayer Process and bauxite calcination method, J. Hazard. Mater. 146 (2007) 255–261.

[32] A. Atasoy, The comparison of the Bayer process wastes on the base of chemical and physical properties, J. Therm. Anal. Calorim. 90 (2007) 153–158.

[33] A. Alp, M.S. Goral, Thermal properties of red mud, J. Therm. Anal. Calorim. 73 (2003) 201–207.

[34] P. Li, D.E. Miser, S. Rabiei, R.T. Yadav, M.R. Hajaligol, The removal of carbon monoxide by iron oxide nanoparticles, Appl. Catal. B: Environ. 43 (2003) 151–162.

[35] Q. Liu, L.C. Wang, M. Chen, Y. Cao, H.Y. He, K.N. Fan, Dry citrate-precursor synthesized nanocrystalline cobalt oxide as highly active catalyst for total oxidation of propane, J. Catal. 263 (2009) 104–113.

[36] T. Glinrun, O. Mekasuwandumrong, J. Panpranot, C. Chaisuk, P. Praserthdam, Improvement of propane oxidation activity over Pt/Al_2O_3 by the use of MIXED γ- and χ-Al_2O_3 supports, React. Kinet. Mech. Catal. 100 (2010) 441–448.